

Supporting Information

Stability, durability and regeneration ability of a novel Ag-based photocatalyst $\text{Ag}_2\text{Nb}_4\text{O}_{11}$

Hongjun Dong,^{a, b} Gang Chen,^{*a} Jingxue Sun,^a Yujie Feng,^{*c} Chunmei Li,^a and Chade Lv^a

a Department of Chemistry, Harbin Institute of Technology, Harbin 150001, P. R. China.

b Department of Chemistry, Baicheng Normal University, Baicheng 137000, P. R. China.

c State Key Laboratory of Urban Water Resource and Environment, Harbin Institute of Technology, Harbin 150090, P. R. China.

Experimental method

1. Synthesis

$\text{Ag}_2\text{Nb}_4\text{O}_{11}$ was synthesized using typical solid phase reaction method. AgNO_3 and Nb_2O_5 were weighed out in an appropriate stoichiometric ratio and ground together in mortar until the mixture was homogeneous mixing. The mixture was then placed in a corundum crucible and heated at 500 °C in an electric furnace in the air. After heating 5 h, the sample was removed and vigorously ground again for 30 min. The precursor was calcined again for an additional 24 h at 800 °C. The white powder was obtained.

2. Characterization

The phases of the $\text{Ag}_2\text{Nb}_4\text{O}_{11}$ sample was characterized by powder X-ray diffractometer (XRD, Rigaku D/max-2000) equipped with a Cu-K α radiation at a scanning rate of 5° min⁻¹ in the 2 θ range of 10-90°. X-ray tube voltage and current were set at 45 kV and 50 mA, respectively. Morphologies of as-prepared samples were characterized utilizing field-emission scanning electron microscopy (FESEM, MX2600FESEM) and transmission electron microscopy (TEM, FEI, Tecnai G2 S-Twin). X-ray photoelectron spectroscopy (XPS) analysis was measured on an American electronics physical HI5700ESCA system with X-ray photoelectron spectroscope using Al K α (1486.6 eV) monochromatic X-ray radiation. The peak positions were corrected against the C 1s peak (284.6 eV) of contaminated carbon. The ultraviolet-visible diffuse reflectance spectra (UV-vis DRS) of the samples were recorded on a UV-vis spectrophotometer (PG, TU-1901) at room temperature with BaSO_4 as the background at 200-900 nm. The nitrogen adsorption and desorption isotherm and Brunauer-Emmett-Teller (BET) specific surface area were measured at 77K using an AUTOSORB-1 Surface Area and Pore Size Analyzer.

3. Photocatalytic characteristics

The degradations of the organic dyes were carried out with 0.5 g catalyst suspended in the rhodamine B (RhB), methylene blue (MB) or methyl orange (MO) solutions (10 mg L⁻¹, 100 ml) with 0.1 ml H₂O₂. Then the degradation reaction system was irradiated with a 300W Xe arc lamp providing UV-visible light. Before the suspensions were irradiated, they were carried out about 2 min of ultrasonic process and magnetically stirred for 50 min in the dark to complete the adsorption-desorption equilibrium between dyes and catalysts. Lastly, the above suspensions were exposed to UV-visible light irradiation under magnetic stirring. UV-vis spectrophotometer (PG, TU-1901) monitored the absorbance of dye solutions at intervals of 5 min. Before measurement,

the catalyst was removed from the reaction system by centrifugalization. The circle operations were carried out using 0.5 g catalyst, and 0.025g catalyst (5%) was added into the reaction system to compensate for the loss of catalyst every performing circle of 10 times.

4. Photoelectrochemical measurements

The photoelectrochemical characteristics were measured in a CHI604C electrochemical working station using a standard three-compartment cell. Catalyst coated FTO glass, a piece of Pt sheet, a Ag/AgCl electrode and 0.5 M sodium sulfate were used as the working electrode, counter-electrode, reference electrode and electrolyte, respectively.

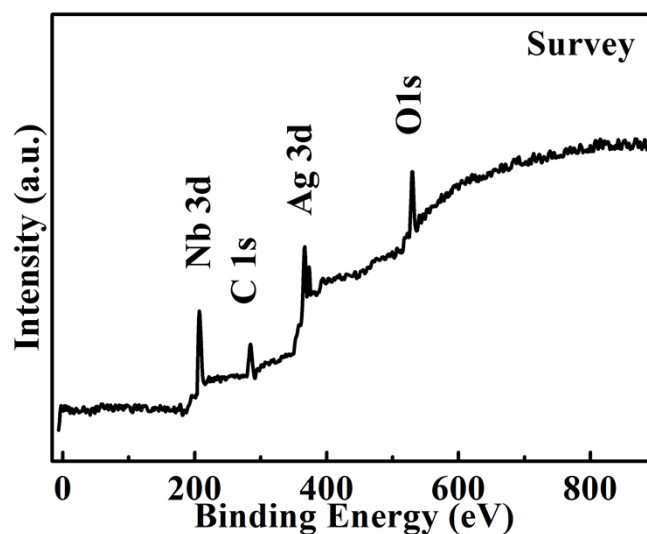


Fig. S1 Survey XPS spectrum of the $\text{Ag}_2\text{Nb}_4\text{O}_{11}$ sample.

Table S1 Surface atomic ratio of the $\text{Ag}_2\text{Nb}_4\text{O}_{11}$ sample

Semiconductor	Ag	Nb	O
$\text{Ag}_2\text{Nb}_4\text{O}_{11}$	12.57	23.71	63.72

The band edge of the crystalline semiconductor can be estimated according to the equations $ah\nu=A(h\nu-E_g)^{n/2}$,¹ in which a , ν , A and E_g are absorption coefficient, light frequency, proportionality constant and band gap, respectively. $n=1$ and $n=4$ decide the characteristics of the direct and indirect transition absorption in a semiconductor. The value of n and E_g is determined by the following steps: first, plot $\ln(ah\nu)$ vs $\ln(h\nu-E_g)$, using the approximate E_g value of 3.21 eV for $\text{Ag}_2\text{Nb}_4\text{O}_{11}$ in accordance of absorption spectra, and then determine the value of n with the slope of the straightest line near the band edge; second, plot $(ah\nu)^{2/n}$ vs $h\nu$ and then evaluate the band gap E_g by extrapolating the straight line to the $h\nu$ axis intercept. We deduce the slope of $\text{Ag}_2\text{Nb}_4\text{O}_{11}$ is approximate equal to 1 and the corresponding value of n may be determined to 2. $\text{Ag}_2\text{Nb}_4\text{O}_{11}$ exhibits not only the indirect but also direct characteristics. Therefore, when $n = 4$ and $n = 1$, the indirect and direct band gaps of $\text{Ag}_2\text{Nb}_4\text{O}_{11}$ are 3.09 eV, and 3.30 eV respectively.² The plots of $\ln(ah\nu)$ vs $\ln(h\nu-3.21)$ and $(ah\nu)^{2/n}$ vs $h\nu$ are shown in Figure S2.

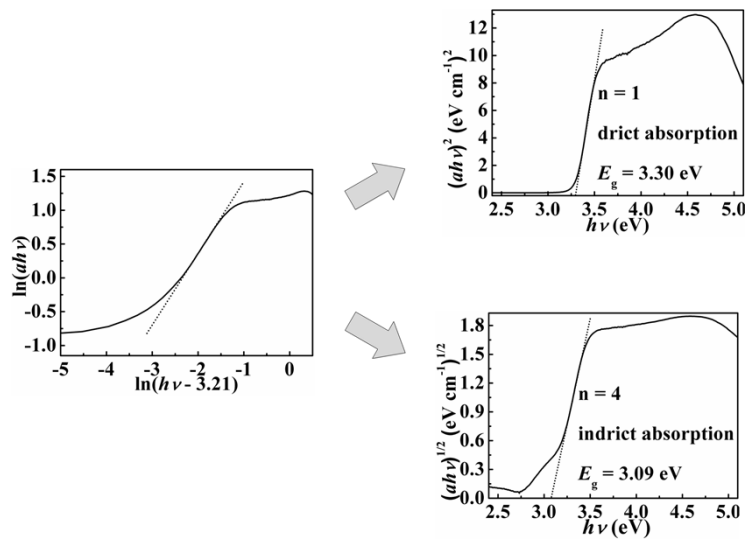


Fig. S2 The plots of $\ln(ah\nu)$ vs $\ln(h\nu - 3.21)$ and $(ah\nu)^{2/n}$ vs $h\nu$.

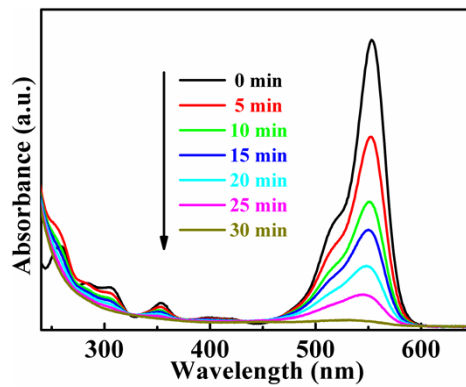


Fig. S3 Absorbance variation of RhB solutions over $\text{Ag}_2\text{Nb}_4\text{O}_{11}$ photocatalyst.

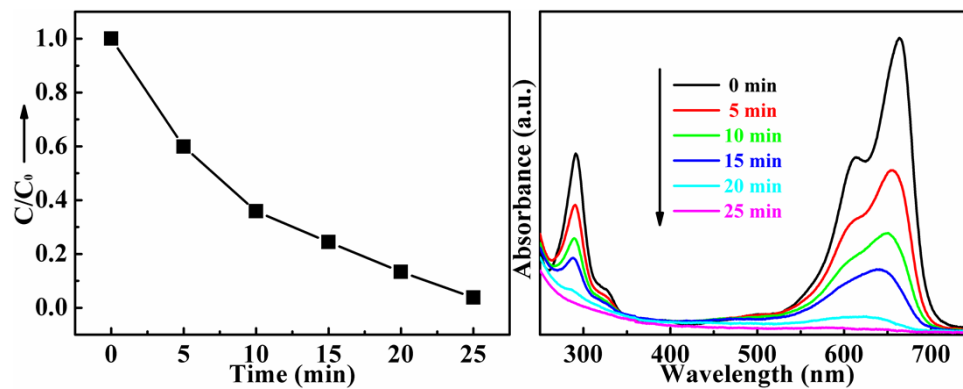


Fig. S4 Dynamic curves (left) and absorbance variation (right) of MB solutions over $\text{Ag}_2\text{Nb}_4\text{O}_{11}$ photocatalyst.

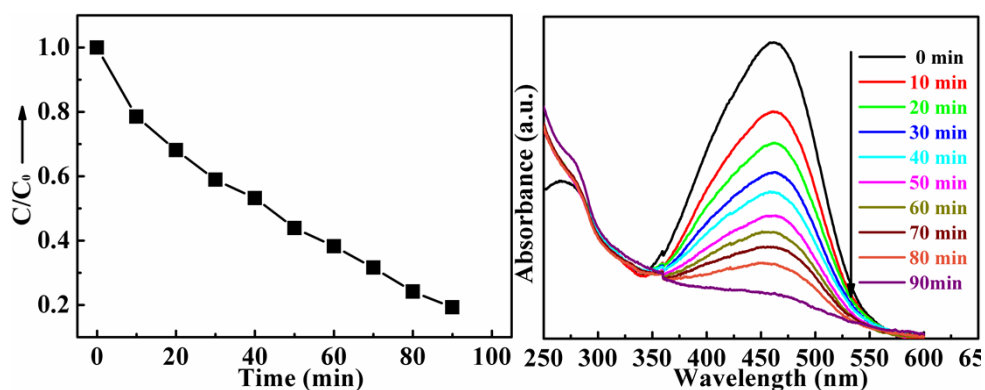


Fig. S5 Dynamic curves (left) and absorbance variation (right) of MO solutions over $\text{Ag}_2\text{Nb}_4\text{O}_{11}$ photocatalyst.

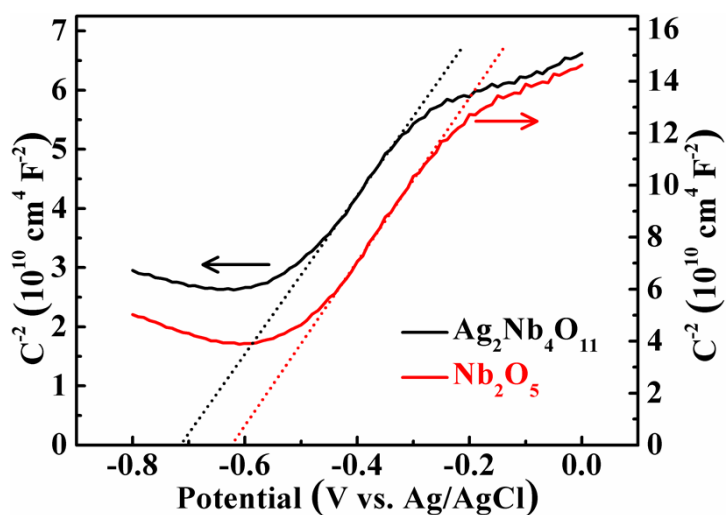


Fig. S6 Mott-Schottky plots of $\text{Ag}_2\text{Nb}_4\text{O}_{11}$ and Nb_2O_5 as electrodes.

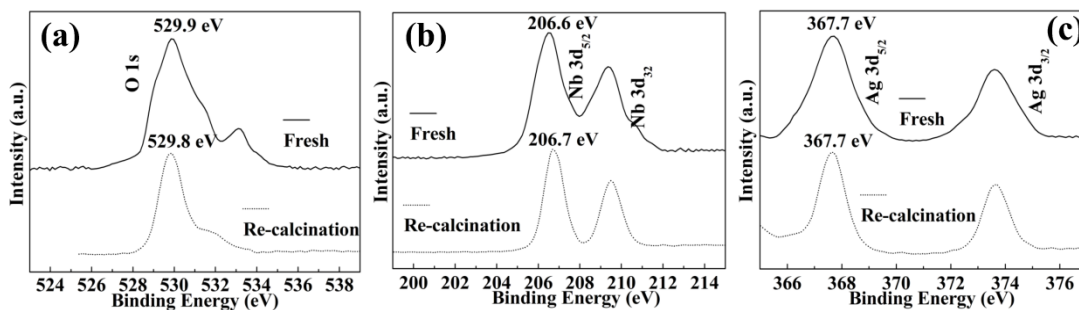


Fig. S7 XPS spectra of the fresh and re-calcination $\text{Ag}_2\text{Nb}_4\text{O}_{11}$ sample

The band positions of Ag₂Nb₄O₁₁ and Nb₂O₅ can be calculated by the following empirical formulae:

$$E_{CB} = X - E_c - 1/2E_g$$

$$E_{VB} = E_{CB} + E_g$$

where X is the absolute electronegativity of the atom semiconductor, expressed as the geometric mean of the absolute electronegativity of the constituent atoms, which is defined as the arithmetic mean of the atomic electron affinity and the first ionization energy; E_c is the energy of free electrons of the hydrogenscale (4.5 eV); E_g is the band gap of the semiconductor; E_{CB} is the conduction band potential and E_{VB} is the valence band potential. The values of X , E_g , CB, and VB of Ag₂Nb₄O₁₁ and Nb₂O₅ samples are shown in Table S2.

Table S2 X , E_g , CB, and VB of Ag₂Nb₄O₁₁ and Nb₂O₅ samples

Semiconductor	X (eV)	E_g (eV)	CB(eV)	VB(eV)
Nb ₂ O ₅	6.21	3.30	0.06	3.36
Ag ₂ Nb ₄ O ₁₁	6.04	3.09	-0.01	3.08

The theoretical calculation is performed based on ab initio density functional theory (DFT).³ Exchange-correlation effects were taken into account by using the GGA (generalized gradient approximation) function of PBE (Perdew, Burke and Ernzerhof).⁴ The band structure and the density of states calculations were performed using the CASTEP code program package,⁵⁻⁶ which utilized pseudo-potentials to describe electron-ion interactions and represented electronic wave functions using a plane-wave basis set. The kinetic energy cutoff was set at 300 eV. The Brillouin-zone sampling was performed by using a k-grid of 4×4×2 points for the calculations.

Reference

- 1 Butler, M. A. Photoelectrolysis and physical properties of the semiconducting electrode WO₃, *J. Appl. Phys.*, 1977, **48**, 1914-1920.
- 2 Z. G. Yi, J. H. Ye, N. Kikugawa, T. Kako, S. X. Ouyang, H. Stuart-Williams, H. Yang, J. Y. Cao, W. J. Luo, Z. S. Li, Y. Liu and R. L. Withers, An orthophosphate semiconductor with photooxidation properties under visible-light irradiation., *Nat. Mater.*, 2010, **9**, 559-563.
3. W. Kohn and L. Sham, Self-Consistent Equations Including Exchange and Correlation Effects, *J. Phys. Rev. A: At. Mol. Opt. Phys.*, 1965, **140**, 1133-1138.
4. M. D. Segall, P. J. D. Lindan, M. J. Probert, C. J. Pickard, P. J. Hasnip, S. J. Clark and M. C. Payne, First-principles simulation: ideas, illustrations and the CASTEP code, *J. Phys. Condens. Matter.*, 2002, **14**, 2717-2744.
5. S. J. Clark, M. D. Segall, C. J. Pickard, P. J. Hasnip, M. J. Probert, K. Refson and M. C. Payne, First principles methods using CASTEP, *Z. Krystallogr.* 2005, **220**, 567-570.
6. J. P. Perdew, K. Burke and M. Ernzerhof, Generalized Gradient Approximation Made Simple, *Phys. Rev. Lett.*, 1996, **77**, 3865-3868.